Quantitative dynamic evolution of physiological parameters of RBC by highly stable digital holographic microscopy

Kumar, Manoj ; Matoba, Osamu ; Quan, Xiangyu ; Rajput, K Sudheesh ; Morita, Mitsuhiro ; Awatsuji, Yasuhiro

(Citation)
Optics and Lasers in Engineering,151:106887

(Issue Date)
2021-12-10

(Resource Type)
journal article

(Version)
Accepted Manuscript

Highlights

1. The evaluation of morphological, quantitative parameters, and membrane fluctuations of human red blood cells (RBC) by a new single-shot common-path off-axis digital holographic microscopic system is demonstrated.
2. The proposed system, owing to common-path configuration, offers higher phase temporal phase stability, therefore, making it more suitable for the investigation of small cell thickness fluctuation.
3. The experimentally calculated parameters of the RBC are obtained in good agreement with their normal physiological range.
4. The system could further be used for quantifying the dynamically changing molecular concentrations and morphology of other non-red blood and living cells.

Quantitative Dynamic Evolution of Physiological Parameters of RBC by Highly Stable Digital Holographic Microscopy

Manoj Kumar[1*], Osamu Matoba[1], Xiangyu Quan[1], Sudheesh K Rajput[1], Mitsuhiro Morita[2], and Yasuhiro Awatsuji[3]

[1]Graduate School of System Informatics, Department of System Science, Kobe University, Rokkodai 1-1, Nada, Kobe 657-8501, Japan
[2]Graduate School of Sciences, Department of Biology, Kobe University, Rokkodai 1-1, Nada, Kobe 657-8501, Japan
[3]Faculty of Electrical Engineering and Electronics, Kyoto Institute of Technology, Matsugasaki, Sakyo-ku, Kyoto 606-8585, Japan
*E-mail: manojklakra@gmail.com

Abstract

Digital holographic microscopy (DHM) is a powerful label-free imaging tool that provides three-dimensional (3D) quantitative information of a specimen. In this work, the evaluation of morphological and quantitative parameters of human red blood cells (RBC) by a new single-shot common-path off-axis digital holographic microscopic system is demonstrated. The proposed system is accomplished by employing a wedge plat, silver-coated at its back surface, into the object beam path generating two beams: one from the front surface and another from the back surface of the wedge plate. One of the beams is spatially filtered by using a pinhole to completely erase the object information from it and serving the clean reference beam, which on interfering with the object beam, creates the hologram. The proposed system, owing to common-path configuration, offers higher temporal phase stability, therefore, making it more suitable for the investigation of small cell thickness fluctuation. Moreover, the system is simple, compact, less expensive, and less vibration sensitive. The measurements of morphological and quantitative parameters, and membrane fluctuations of the human RBCs by the proposed system are reported. The experimentally calculated parameters of the RBC are obtained in good agreement with their normal physiological range.

Keywords: digital holographic microscopy, quantitative phase, morphological and quantitative parameters, red blood cells.

---

1. Introduction

Biophysical parameters of the biological cells and tissues such as morphology, refractive index, thickness, cell dry mass, density, hemoglobin concentration, etc. play important role in determining and understanding of various physiological and pathological processes, monitoring of disease progression, and therefore, helpful in their improved diagnosis [1-7]. The biological specimens, e.g., living cells and their intracellular constituents, are considered as phase objects as they are mostly transparent in the visible

range. Therefore, investigations of these biological specimens by conventional bright-field microscopy are uncertain as it does not provide quantitative information about the cell structure and contents and therefore, requires additional efforts for this purpose. Some external interventions, such as chromatographic agents or fluorescent markers, are employed for the analysis of these specimens [8]. Several techniques including phase-contrast microscopy and differential interference contrast, have been developed over the years to avoid these external interventions. Among them, quantitative phase imaging (QPI) by digital holographic microscopy (DHM), being a label-free, non-invasive, and highly sensitive technique to visualize and measure subtle, is the forefront as a promising tool in the determination of various biophysical parameters and quantitative characterization of the biological cells and tissues [9]. DHM has been established as a powerful technique in the field of biomedical imaging and analysis including the single-cell studies for the analysis of blood [10], endothelial [11] and neuronal cells [12], cancer cell research [13], fibroblast cells [14], testate amoeba [15], diatom skeletons [16], infections [17], cell culture quality control [18,19], the histopathological analysis of tissue samples [20], and others [21].

Red blood cells (RBCs) are an essential component of the human body. The role of the RBCs is to deliver fresh oxygen to the body tissues via blood flow through the circulatory system in vertebrate organisms while squeezing through the body's capillaries and transporting carbon dioxide from tissues to the lungs for the human to exhale [22,23]. The shape of the RBCs is round with a flattish, indented center, similar to doughnuts without a hole. The RBCs are made in the bone marrow and their typical life cycle is about 120 days [24]. Foods rich in iron and vitamins (B-2, B-3, and B-12) help to maintain healthy RBCs. Several biochemical, structural, inflammatory, and physiologic changes occur in stored RBCs - when the RBCs store for a substantial amount of time, referred RBC storage lesion, which affects directly or indirectly other body tissues. In RBC storage lesion, over time, glucose in stored blood is consumed and the potassium levels increase [24]. Therefore, the investigations of various quantitative cell parameters including 3D morphology, mean corpuscular volume (MCV), hemoglobin content (MCH), MCH surface density (MCHSD), of RBCs provide useful information which helps in improving the deeper understanding of the mechanisms behind human diseases. For example, anemias are diseases characterized by low oxygen transport capacity of the blood, due to the low red cell count or some abnormality of the RBCs such as the small size of the RBCs or the hemoglobin. Therefore, the larger volume or the size of the RBCs leads to the transport of more oxygen and hence they are good indicators of the functionality of RBCs.

DHM is one of the powerful optical microscopic techniques which has been actively investigated and widely used for such applications with its unique advantages over conventional techniques. In the recent decade, the common-path configurations of DHM are of growing interest because they have overcome the limitations of the two-channel configurations and make the systems simpler, compact in size, inexpensive due to reduced optical components, less vibration-sensitive, and provide high temporal phase stability [4,5,7,25-33]. Recently, we have developed a common-path configuration of DHM based on a cube beam splitter and demonstrated its applications for bio-imaging [7] and simultaneous measurement of refractive index and thickness of a biological specimen [34] and its various applications [35]. However, in this system, there is limited control on the complex conjugate terms in the spatial frequency domain of the recorded hologram.

In the present work, we have developed a new configuration of the common-path off-axis DHM system based on a wedge plate coated at its back surface. The wedged glass plate-based DHM system for bio-imaging applications is proposed by Sun et al [36] in which the wedged glass plate is inserted, in the path of the collimated incident object beam where object information is not present, acts as the reference beam,

to deflect this half of the object beam toward another half where the object information is present. The interference between the two halves is occurred to generate an off-axis hologram. However, in this configuration, the sample under study is occupying only half of the object beam, and therefore, it reduces the overall field of view (FOV) by half. Furthermore, if the object information is occupied in the entire object beam, then the technique does not work, limits its use for small objects only. Also, it is tricky to identify where the object information and no object information are present in the object beam and then to insert the wedge plate accordingly to generate the interference pattern. The system is not suitable for the investigations of dynamic events. On the other hand, in our system, the object beam is reflected from the front and back surfaces of a wedge plate, where one of the beams is spatially filtered at its Fourier plane using a pinhole to generate a spherical reference beam free from the object information. This reference beam interferes with the object beam at the faceplate of the image sensor and forms the digital hologram. Therefore, the full use of the object beam is utilized and the problem of reduced FOV is overcome. The proposed system is used for the investigations of various quantitative cell parameters of the RBCs. In the following section, the methodology of the proposed system is presented. In the third section, the analysis of the experimental results is demonstrated. In the final section, the discussion and conclusion of the study are presented.

2. Methodology

Figure 1(a) shows the schematic of the experimental setup of the proposed wedge plate-based single-shot common-path. The wedge plate is silver coated at its back surface. The He-Ne laser, (λ = 632.8 nm) is spatially filtered (by SF) and collimated (by L1). This collimated laser light trans-illuminates the sample mounted on a motorized translational stage. The light transmitted through the sample is collected by a microscopic objective lens (40X magnification, NA = 0.65) and collimated again by the lens (L2 of focal length = 100 mm). The collimated light is focused by the lens, L3 of focal length = 150 mm, and is reflected by the wedge plate (Thorlabs, PS810 - Ø1", round wedge prism, 2° beam deviation). Therefore, two beams: one from the front surface and another from the silver coated back surface of the wedge plate, are generated. Both these beams carry the object information and one of the beams (reflected from the back surface of the wedge plate as its intensity is very high compared to the other) is spatially filtered at its Fourier plane by using a pinhole (50 µm, diameter), mounted on a 3D stage to adjust the right position of the pinhole at the focused spot of the beam. The pinhole allows to pass only the DC component of the beam generates spherical wave by erasing all the object information. The reference and object beams are allowed to pass through a lens (L4 of focal length = 100 mm), to make their interference at the faceplate of the image sensor [CMOS camera (Sony Pregius IMX 249, sensor format: 1920×1200 pixels, pixel size of 5.86 µm)].

However, it should be noted that the setup can be made more compact and simpler by using only the wedge plate without the pinhole by replacing the optical geometry in the dotted area of Fig. 1(a) with the scheme depicted in Fig. 1(b). In this case, the collimated object beam is allowed to incident on the wedge plate and two laterally sheared beams are generated after reflection from the front and rear surfaces of the plate. The portion, not containing any object information, in one of the beams, acts as the reference beam and it interferes with the other beam carrying the object information and generates an interference pattern at the faceplate of the image sensor. This configuration makes the setup more compact and simpler by reducing the number of optical components and the complexity of the pinhole assembly, but at the cost of reduces FOV. This scheme is compatible for the investigations of small biological objects. Further, there is no need for the silver coating of the back surface in this configuration.

A single digital hologram in the presence of the object is recorded from which phase information is retrieved by using the principal component analysis (PCA)-based phase aberration compensation method [37]. This method has several advantages such as it is fully automatic, accurate, robust, and it does not require any prior knowledge of the object or/and the optical setup. From the obtained quantitative phase image, various physiological parameters of the RBC are calculated which have immense importance in defining the several diseases and other functionality of the RBCs.

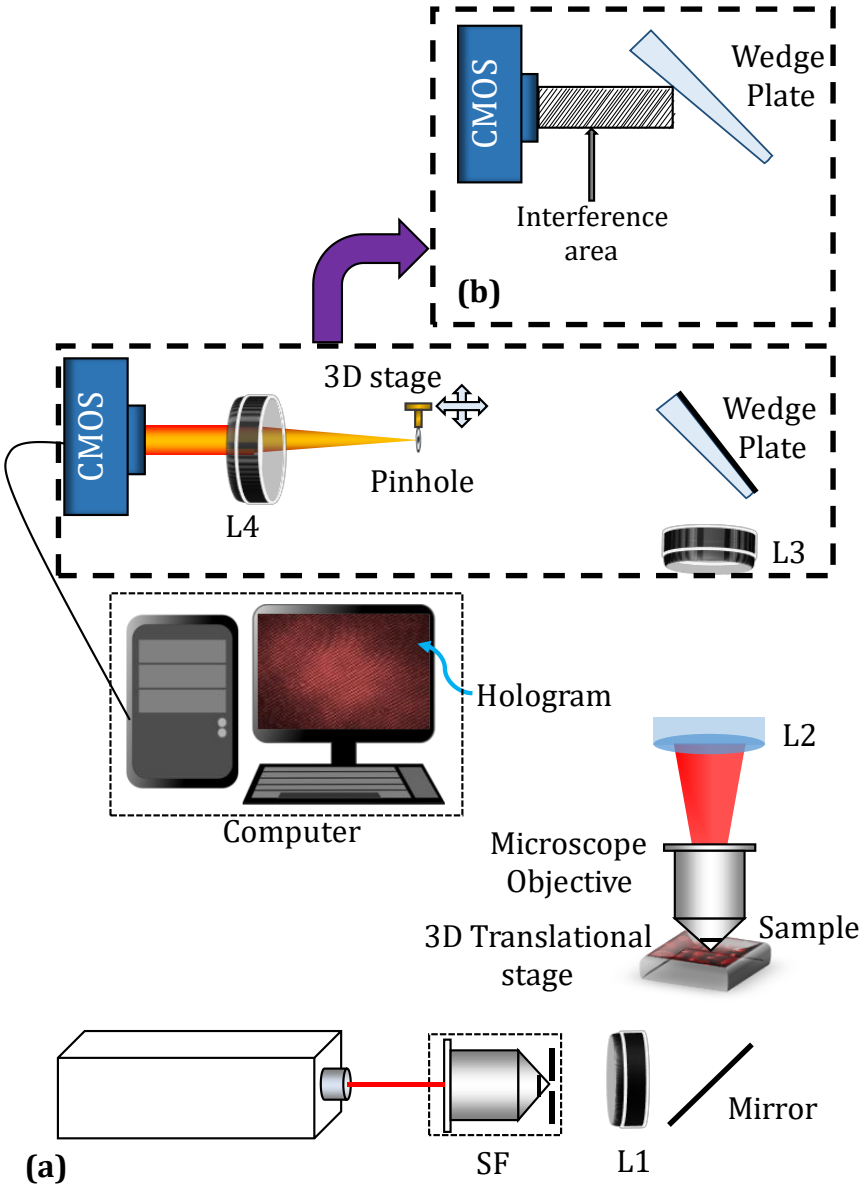

Fig. 1. Schematic of the experimental setup.

3. Experiments and Results

First, the temporal stability of the system is measured by recording a series of holograms, as shown in Fig. 2(a), without the presence of the object, at the rate of 40 frames per second, for 100 s. For all the 4000 holograms, the phase distributions are reconstructed numerically. The phase difference distributions are

calculated for all the holograms by comparing the reconstructed phase distributions to that of the first recorded hologram. The standard deviation of the phase difference for a selected area (10,000 random pixel points) in the same area of every phase difference distribution is calculated. Figure 2(b) shows the histogram of the standard deviation of fluctuations for the selected pixels within the field of view indicating that a mean fluctuation (σ_{mean}) is 0.0047 radians.

Then the experiments were conducted on human red blood cells (RBCs) for quantitative analysis of morphological properties including the mean corpuscular volume (MCV), hemoglobin content (MCH), and MCH surface density (MCHSD). The RBC sample is prepared by collecting a few microliters of blood from a healthy lab donor. The RBC sample was resuspended in phosphate buffer saline containing 1000 unit/L heparin (Wako, Tokyo, Japan)

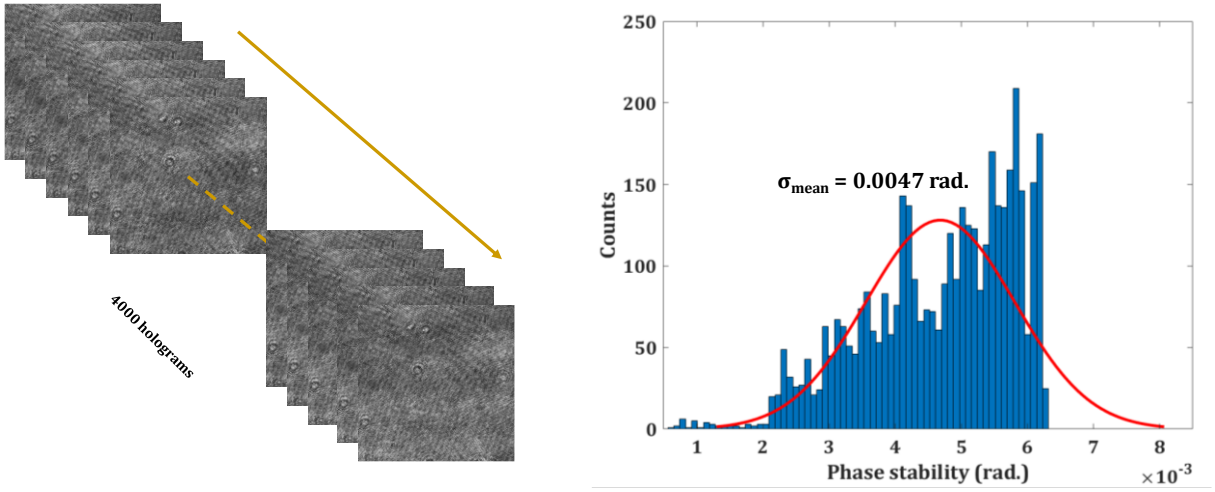

(a) (b)

Fig. 2. (a) Recorded series of holograms and (b) Histogram of standard deviations of fluctuations of the reconstructed phase distributions for the selected pixels, defining the temporal phase stability of the system.

Cell diameter and thickness

Figure 3 (a) shows the recorded digital hologram, where the inset shows the magnified selected area of the recorded hologram clearly indicating the carrier fringe pattern. The quantitative phase information of RBCs is extracted from the recorded digital hologram as shown in Fig 3(b). The diameter of the cell can be calculated either of the intensity or phase image by calculating the total number of pixels and pixel size that a cell occupies in the image. Further, from the phase distribution ($\Delta\phi(x,y)$), the cell thickness is calculated as

$$h(x,y) = \frac{\Delta\phi(x,y)\times\lambda}{2\pi\Delta n}, \quad (1)$$

where, $\Delta n = n_{RBC} - n_m$, with n_{RBC} is the refractive index of the RBC and n_m is the refractive index of the surrounding medium (phosphate buffer) and λ is the wavelength of the light source used in the experiment. The refractive index of RBC and phosphate buffer are ~1.418 and ~1.335, respectively [38]. However, both the thickness and refractive index of the RBC can be accurately calculated by the dual-wavelength DHM system [35]. The thickness profile of the RBC is shown in Fig. 3(c).

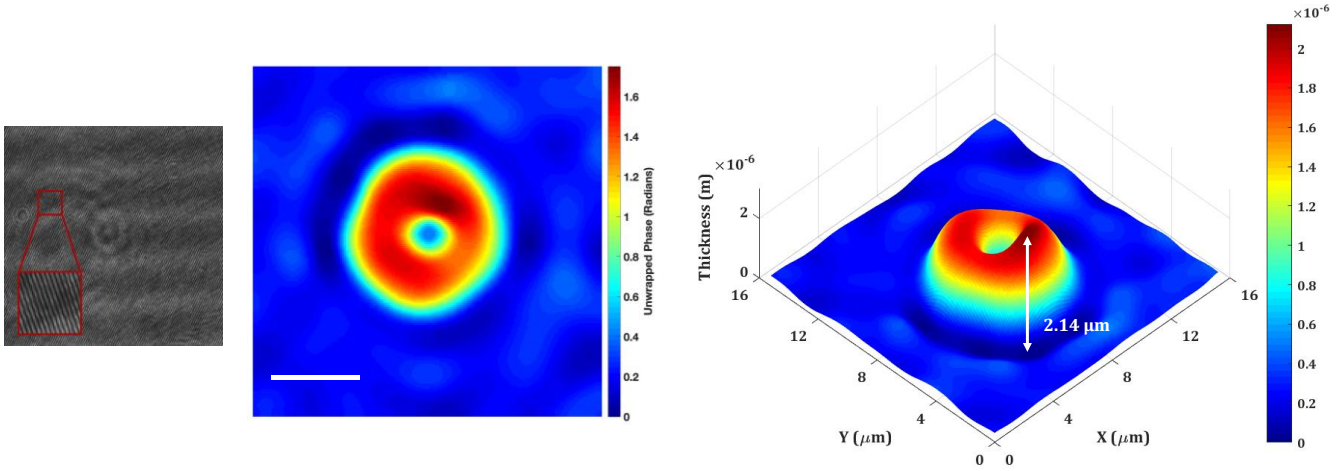

(a) (b) (c)

Fig. 3: (a) Recorded digital hologram, where the inset represents the magnified selected area showing the carrier fringes, scale bar = 5µm, (b) retrieved phase distribution, and (c) the thickness profile of the RBC.

Quantitative and Hemoglobin parameters

The quantitative phase image obtained by the proposed DHM system enables to measure several characteristic properties of the RBC including the mean corpuscular volume (*MCV*), projected surface area (*S*), dry mass (*DM*), or the mean corpuscular hemoglobin concentration (*MCH*) when the RBC population is considered, and mean corpuscular hemoglobin surface density (*MCHSD*) [38-41]. In the *MCV* blood test, the average size of the RBCs is measured. If the size of the RBCs is too small or too large, it may be a sign of a blood disorder including anemia or a vitamin deficiency. The abnormal hemoglobin concentration results in sickle-cell disease because in this case the when these release their oxygen load to the tissues, they become insoluble and leading to misshaped RBCs. These sickle-shaped RBCs cause various diseases such as blood vessel blockage, strokes, tissue damage, and pain because they are less deformable and viscoelastic.

These properties of the RBC are related to the average phase and the projected surface area of the RBC. Therefore, the average phase value, Φ induced by the whole RBC, is calculated by the following equation [38-41],

$$\Phi = \frac{1}{N}\sum_{i=1}^{N}\Delta\phi_i \,, \tag{2}$$

where, N is the total number of pixels in the RBC and $\Delta\phi_i$ is the phase value of each pixel within the RBC.

The projected surface area (S) of the RBC is measured as [38-41],

$$S = Np^2 \,, \tag{3}$$

where, p is the pixel size in the quantitative phase image.

The volume of a single RBC is defined as [38-41],

$$V = \frac{p^2\lambda}{2\pi\Delta n}\sum_{i=1}^{N}\Delta\phi_i \,, \tag{4}$$

When a population of RBCs is considered, then the above equation [Eq. (4)] is used to measure the *MCV*.

The dry mass (*DM*), which measures the weight of the cell after dehydration, is an important characteristic of the RBC, which is used to compare cells [39]. The *DM* of a cell is defined as [38-41]

$$DM = \frac{10\lambda S}{2\pi\alpha}\sum_{i=1}^{N}\Delta\phi_i \,, \tag{5}$$

where, α is the specific refraction increment constant related mainly to the protein concentration (0.00196 m^3/kg for λ = 632.8 nm). The *MCH* is obtained when the RBC population is considered as it is used as an important parameter for the investigation of change in the hemoglobin content in the RBCs [39]. The mean corpuscular hemoglobin surface density (*MCHSD*), an indicator of the hemoglobin concentration in the RBC, can be calculated from the *MCH* and *S* as follows,

$$MCHSD = \frac{MCH}{S}\,. \tag{6}$$

From the obtained quantitative phase image (Fig. 3(b)), these parameters are measured by using the equations discussed above. The calculated values of these parameters are listed in Table 1 which are in good agreement with their normal physiological range.

Table 1: Calculated and normal range values of the parameters.

S. No.	Parameters	Calculated Values	Normal range
1	Diameter	7.98 µm	~ 6.2 – 8.2 µm [42]
2	*h*	2.14 µm	~ 1.7 – 2.2 µm [42]
3	*S*	44.62 μm^2	~ 25-50 μm^2 [39]
4	*V*	98.52 fl	~ 80 – 99 fl [41]
5	*DM*	27.57 pg	~ 27-31 pg [41]

h = cell thickness, *S* = projected surface area, *V* = cell volume, *DM* = dry mass,

Membrane Fluctuation of Cell

The RBC membrane is elastic which is a metabolically regulated active structure and its static and dynamic characteristics are controlled by biochemical energy. The dynamics of the RBC membrane is related to the membrane structure and mechanical properties. The membrane fluctuation rate is calculated in terms of temporal thickness variation from the video holograms recorded for about 6 seconds with a frame rate of 30 fps. Then each video hologram frame is numerically reconstructed to obtain the time-varying thickness profile of the cell. The measured standard deviations for one pixel over the time on the ring (point A, in Fig. 4), at the center (point B) in the doughnut shape, and outside the cell in the background (point C) are 37.97, 28.38, and 21.11 nm, respectively, indicating that the membrane fluctuation amplitudes are significantly larger than the background and center levels.

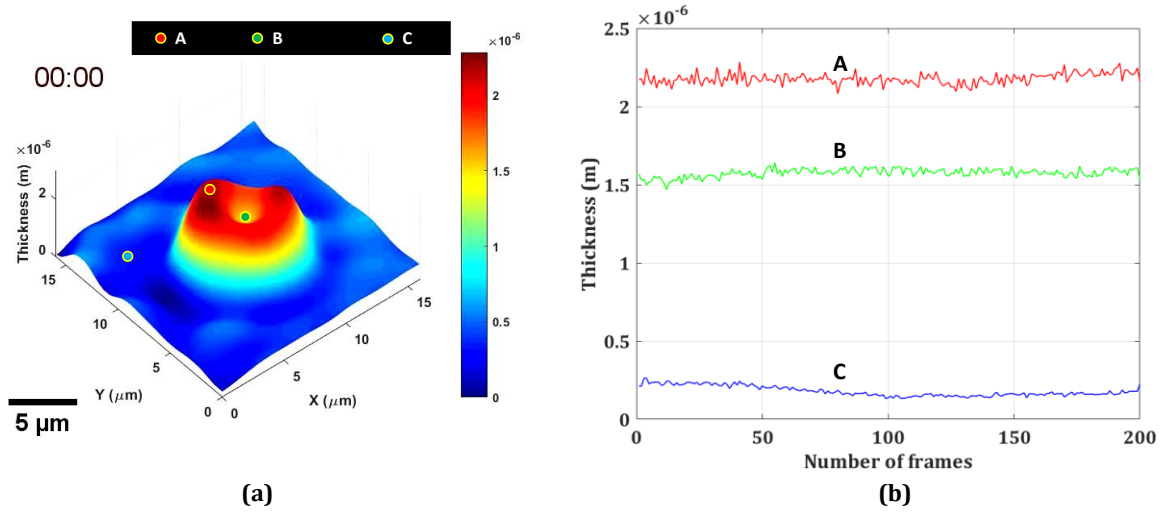

(a) (b)

Fig. 4 (a): Thickness profile of a single RBC and (b) thickness fluctuation over time at three locations (A, B, and C) indicated in (a) at the ring, center, and outside of the RBC.

4. Conclusion

In this work, we have developed a new off-axis common-path DHM system based on a wedge plate, and because of the common-path configuration of the system, it provides several advantages over the two-channel configurations of DHM systems which makes it a suitable candidate for a wide range of biological inspection and optical measurement applications. The system is used for the investigation of the 3D morphology and other physiological parameters such as volume, projected surface area, dry mass of the human RBC. The dynamic membrane fluctuation and the Hb concentration of individual RBCs are measured. The obtained results are found in good agreement with their normal physiological range. The system could further be used for quantifying the dynamically changing molecular concentrations and morphology of other non-red blood and living cells. The proposed DHM system could be a promising tool for medical diagnostics and analysis and other biological applications.

Acknowledgments

Core Research for Evolutional Science and Technology (JPMJCR1755); Japan Society for the Promotion of Science (16J05689, 18H03888).

Declaration of Competing Interest

This paper has no Conflict of interest.

References

[1] P. Marquet, B. Rappaz, P. J. Magistretti, E. Cuche, Y. Emery, T. Colomb, and C. Depeursinge, Digital holographic microscopy: a noninvasive contrast imaging technique allowing quantitative visualization of living cells with subwavelength axial accuracy, Opt. Lett., 30, 468–470 (2005).

[2] B. Rappaz, P. Marquet, E. Cuche, Y. Emery, C. Depeursinge, P. Magistretti, “Measurement of the integral refractive index and dynamic cell morphometry of living cells with digital holographic microscopy,” Opt. Express 13(23), 9361-9373. (2005).

[3] B. Rappaz, E. Cano, T. Colomb, J. Kuhn, C. Depeursinge, V. Simanis, P. J. Magistretti, P. Marquet, “Noninvasive characterization of the fission yeast cell cycle by monitoring dry mass with digital holographic microscopy,” J. Biomed. Opt. 14(3), 034049 (2009).
[4] B. Kemper, A. Vollmer, G. von Bally, C. E. Rommel, and J. Schnekenburger, “Simplified approach for quantitative digital holographic phase contrast imaging of living cells," J. Biomed. Opt. 16(2), 026014 (2011).
[5] N. T. Shaked, “Quantitative phase microscopy of biological samples using a portable interferometer,” Opt. Lett. 37(11), 2016-2018 (2012).
[6] S. Aknoun, J. Savatier, P. Bon, F. Galland, L. Abdeladim, B. F. Wattellier, and S. Monneret, “Living cell dry mass measurement using quantitative phase imaging with quadriwave lateral shearing interferometry: an accuracy and sensitivity discussion,” J. Biomed. Opt. 20(12), 126009 (2015).
[7] M. Kumar, X. Quan, Y. Awatsuji, C. Cheng, M. Hasebe, Y. Tamada, and O. Matoba, “Common-path multimodal three-dimensional fluorescence and phase imaging system,” Journal of Biomedical Optics, 25(3), 032010 (2020).
[8] M. Mihailescu, I. A. Paun, E. Vasile, R. C. Popescu, A. V. Baluta, and D. G. Rotaru, “Digital off-axis holographic microscopy: from cells vizualization, to phase shift values, ending with physiological parameters evolution,” Rom. J. Phys. 61, 1009–1027 (2016).
[9] G. Popescu, Quantitative Phase Imaging of Cells and Tissues (McGraw-Hill, New York, 2011).
[10] Y. Park, T. Yamauchi, W. Choi, R. Dasari, and M. S. Feld, “Spectroscopic phase microscopy for quantifying hemoglobin concentrationsin intact red blood cells,” Opt Lett 34, 3668–3670, (2009).
[11] W.Seo, E. Seo, and S. J. Lee, “Cellular imaging using phase holographic microscopy: for the study of pathophysiology of red blood cells and human umbilical vein endothelial cells,” Journal of Visualization 17, 235–244 (2014).
[12] S. A. Yang, J. Yoon, K. Kim, and Y. Park, “Measurements of morphological and biophysical alterations in individual neuron cells associated with early neurotoxic effects in Parkinson’s disease,” Cytometry A 91, 510–518, (2017).
[13] B. Kemper, et al. “Investigation of living pancreas tumor cells by digital holographic microscopy,” J Biomed Opt 11, 34005, (2006).
[14] C.J. Mann, L.F. Yu, and M.K. Kim, “Movies of cellular and sub-cellular motion by digital holographic microscopy,” Biomed. Eng. Online 5: 21 (2006).
[15] F. Charriere, N. Pavillon, T. Colomb, C. Depeursinge, T.J. Heger, E.A.D. Mitchell, P. Marquet, and B. Rappaz, “Living specimen tomography by digital holographic microscopy: morphometry of testate amoeba,” Opt. Express 14, 7005–7013 (2006).
[16] M. Debailleul, B. Simon, V. Georges, O. Haeberle, and V. Lauer, “Holographic microscopy and diffractive microtomography of transparent samples,” Meas. Sci. Technol. 19, 074009 (2008).
[17] A. E. Ekpenyong, et al. “Bacterial infection of macrophages induces decrease in refractive index,” J Biophotonics 6, 393–397, (2013).
[18] L. Kastl, M. Isbach, D. Dirksen, J. Schnekenburger, and B. Kemper, “Quantitative phase imaging for cell culture quality control,” Cytometry A 91(5), 470-481 (2017).
[19] D. Bettenworth, et al. “Quantitative phase microscopy for evaluation of intestinal inflammation and wound healing utilizing label free biophysical markers,” Histol Histopathol 33, 417–432, (2018).
[20] P. Lenz, et al. “Digital holographic microscopy quantifies the degree of inflammation in experimental colitis,” Integr Biol (Camb) 5, 624–630, (2013).
[21] M. Kumar, X. Quan, Y. Awatsuji, Y. Tamada, and O. Matoba, “Digital holographic multimodal cross-sectional fluorescence and quantitative phase imaging system,” Sci. Rep. 10(1), 1-13 (2020).
[22] F. Yi, I. Moon, and Y. H. Lee, “Three-dimensional counting of morphologically normal human red blood cells via digital holographic microscopy,” J. Biomed. Opt. 20(1), 016005 (2015).
[23] Yi, F., Moon, I., & Javidi, B. (2016). Cell morphology-based classification of red blood cells using holographic imaging informatics. Biomedical Optics Express, 7(6), 2385-2399.
[24] D. B. Kim-Shapiro, J. Lee, and M. T. Gladwin, “Storage lesion: role of red blood cell breakdown,” Transfusion, 51(4), 844-851 (2011).
[25] G. Popescu, T. Ikeda, R. R. Dasari, and M. S. Feld, “Diffraction phase microscopy for quantifying cell structure and dynamics,” Optics letters 31(6), 775-777 (2006)
[26] P. Bon et al., “Quadriwave lateral shearing interferometry for quantitative phase microscopy of living cells,” Opt. Express 17, 13080–13094 (2009).
[27] W. Qu, K. Bhattacharya, C.O. Choo, Y. Yu and A. Asundi, “Transmission digital holographic microscopy based on a beam-splitter cube interferometer,” Appl. Opt. 48, 2778 (2009).

[28] J. Jang, C. Y. Bae, J.-K. Park, and J. C. Ye, "Self-reference quantitative phase microscopy for microfluidic devices," Optics letters 35(4), 514-516 (2010).
[29] A. Calabuig, M. Matrecano, M. Paturzo, and P. Ferraro, "Common-path configuration in total internal reflection digital holography microscopy," Optics letters 39(8), 2471-2474 (2014).
[30] W.-C. Hsu, J.-W. Su, T.-Y. Tseng, and K.-B. Sung, "Tomographic diffractive microscopy of living cells based on a common-path configuration," Optics letters 39(7), 2210-2213 (2014).
[31] S. Mahajan, V. Trivedi, P. Vora, V. Chhaniwal, B. Javidi, and A. Anand, "Highly stable digital holographic microscope using Sagnac interferometer," Optics letters 40(16), 3743-3746 (2015).
[32] S. Ebrahimi, M. Dashtdar, E. Sanchez-Ortiga, M. Martinez-Corral, and B. Javidi, "Stable and simple quantitative phasecontrast imaging by Fresnel biprism," Appl. Phys. Lett.112, 113701 (2018).
[33] J. Běhal, "Quantitative phase imaging in common-path cross-referenced holographic microscopy using double-exposure method," Scientific reports, 9(1), 1-7 (2019).
[34] M. Kumar, X. Quan, Y. Awatsuji, Y. Tamada, and O. Matoba, "Single-shot common-path off-axis dual-wavelength digital holographic microscopy," Applied Optics, 59(24), 7144-7152 (2020).
[35] M Kumar, O Matoba, X Quan, SK Rajput, Y Awatsuji, Y Tamada, "Single-shot common-path off-axis digital holography: applications in bioimaging and optical metrology [Invited]," Applied Optics, 60(4), A195-A204 (2021).
[36] T. Sun, Z. Zhuo, W. Zhang, J. Lu, and P. Lu, "Single-shot interference microscopy using a wedged glass plate for quantitative phase imaging of biological cells," Laser Phys. 28 (2018) 125601.
[37] C. Zuo, Q. Chen, W. Qu, and A. Asundi, "Phase aberration compensation in digital holographic microscopy based on principal component analysis," Opt. Lett. 38, 1724-1726 (2013).
[38] K. Jaferzadeh, I. Moon, M. Bardyn, M. Prudent, J. D. Tissot, B. Rappaz, and P. Marquet, "Quantification of stored red blood cell fluctuations by time-lapse holographic cell imaging," Biomedical optics express, 9(10), 4714-4729 (2018).
[39] I. Moon, F. Yi, Y. H. Lee, B. Javidi, D. Boss, and P. Marquet, "Automated quantitative analysis of 3D morphology and mean corpuscular hemoglobin in human red blood cells stored in different periods," Optics express, 21(25), 30947-30957 (2013).
[40] B. Rappaz, E. Cano, T. Colomb, J. Kuhn, C. D. Depeursinge, V. Simanis, P. Marquet, "Noninvasive characterization of the fission yeast cell cycle by monitoring dry mass with digital holographic microscopy," Journal of biomedical optics, 14(3), 034049 (2013).
[41] Y. Jang, J. Jang, and Y. Park, "Dynamic spectroscopic phase microscopy for quantifying hemoglobin concentration and dynamic membrane fluctuation in red blood cells," Optics express, 20(9), 9673-9681 (2012).
[42] M. Diez-Silva, M. Dao, J. Han, C.T. Lim, and S. Suresh, "Shape and biomechanical characteristics of human red blood cells in health and disease," MRS bulletin/Materials Research Society, 35(5), 382 (2010).

Declaration of Competing Interest

This paper has no Conflict of interest.